

Spin temperatures and covering factors for H I 21-cm absorption in damped Lyman- α systems

S. J. Curran^{1*}, M. T. Murphy², Y. M. Pihlström³, J. K. Webb¹, C. R. Purcell¹

¹*School of Physics, University of New South Wales, Sydney NSW 2052, Australia*

²*Institute of Astronomy, Madingley Road, Cambridge CB3 0HA, UK*

³*National Radio Astronomy Observatory, P.O. Box 0, Socorro, NM87801, USA*

Accepted —. Received —; in original form —

ABSTRACT

We investigate the practice of assigning high spin temperatures to damped Lyman- α absorption systems (DLAs) not detected in H I 21-cm absorption. In particular, Kanekar & Chengalur (2003) have attributed the mix of 21-cm detections and non-detections in low redshift ($z_{\text{abs}} \leq 2.04$) DLAs to a mix of spin temperatures, while the non-detections at high redshift were attributed to high spin temperatures. Below $z_{\text{abs}} = 0.9$, where some of the DLA host galaxy morphologies are known, we find that 21-cm absorption is normally detected towards large radio sources when the absorber is known to be associated with a large intermediate (spiral) galaxy. Furthermore, at these redshifts, only one of the six 21-cm non-detections has an optical identification and these DLAs tend to lie along the sight-lines to the largest background radio continuum sources. For these and many of the high redshift DLAs occulting large radio continua, we therefore expect covering factors of less than the assumed/estimated value of unity. This would have the effect of introducing a range of spin temperatures considerably narrower than the current range of $\Delta T_s \gtrsim 9000$ K, while still supporting the hypothesis that the high redshift DLA sample comprises a larger proportion of compact galaxies than the low redshift sample.

Key words: quasars: absorption lines – cosmology: observations – cosmology: early Universe – galaxies: ISM

1 INTRODUCTION

Despite their relative paucity, the highest column density absorption systems, damped Lyman- α systems (where $N_{\text{HI}} \geq 2 \times 10^{20}$ cm⁻²), are an important component of the high redshift ($z \sim 2-6$) Universe since they account for most of the neutral gas available for star formation (e.g. Lanzetta et al. 1991). The H I 21-cm hyperfine transition can provide an alternative and complementary view of DLAs. Presuming that the 21-cm and Lyman- α absorption arise in the same cloud complexes (Dickey & Lockman 1990)¹, the column density [cm⁻²] of the absorbing gas in a homogeneous cloud is related to the velocity integrated optical depth, where $\tau \equiv -\ln(1 - \frac{\sigma}{fS})$, of the 21-cm line via (Wolfe & Burbidge 1975):

$$N_{\text{HI}} = 1.823 \times 10^{18} T_{\text{spin}} \int \tau dv, \quad (1)$$

where T_s [K] is the spin temperature, σ is the depth of the line (or r.m.s. noise in the case of a non-detection) and S and f the flux

density and covering factor of the background continuum source, respectively.

As summarised by Wolfe (1980), 21-cm absorption line studies can face some difficulties compared with optical work: (1) in blind surveys the bandwidth of radio receiver/backend combinations only allows small redshift intervals to be searched for H I absorption; (2) terrestrial interference can be severe below 1.4 GHz; (3) if the spin temperature of the absorbing gas is high or if the background source size exceeds that of the absorption cloud(s), then the apparent optical depth can be considerably overestimated. Despite these technical difficulties, 21-cm studies of DLAs have provided information about the physical conditions of absorbers, including the kinematics, temperature and velocity distribution of the gas.

One unresolved question concerns the typical size and structure of DLAs, with models ranging from large, rapidly rotating proto-disks (e.g. Prochaska & Wolfe 1997) to small, merging subgalactic systems (e.g. Haehnelt, Steinmetz & Rauch 1998). Direct imaging by various groups (e.g. Le Brun et al. 1997; Rao et al. 2003; Chen & Lanzetta 2003) of the low- z DLA host-galaxies reveals a mix of spirals, dwarf and low surface brightness (LSB) galaxies. This ‘mixed morphology’ picture of DLA host-galaxies appears to be reflected in the nearby Universe in a recent 21-cm

* E-mail: sjc@phys.unsw.edu.au

¹ Where the 21-cm and Lyman- α absorption trace the cold and total neutral hydrogen, respectively.

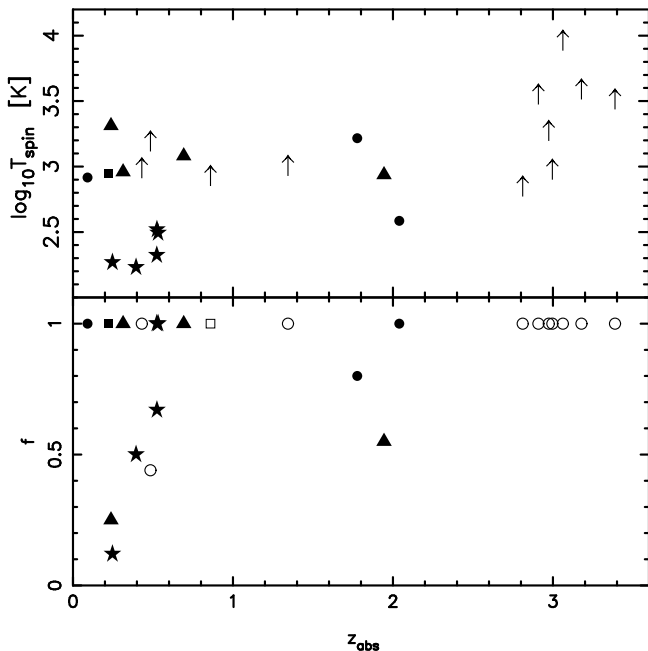


Figure 1. Top: Spin temperature against absorption redshift as given in KC03. The solid symbols represent the 21-cm detections and the shapes represent the type of galaxy with which the DLA is associated: circle–unknown type, star–spiral, square–dwarf, triangle–LSB (obtained from KC03 and references therein). This key is also applied to Figs. 2 to 5. The arrows show the spin temperature lower limits and all of these but one (0454+039 at $z_{\text{abs}} = 0.8596$) have unknown host identifications. Bottom: The covering factors applied to derive the spin temperatures. The shapes are coded as above with the solid and open symbols representing the covering factors applied for the 21-cm detections and non-detections, respectively.

$z = 0$ emission study (Ryan-Weber, Webster & Staveley-Smith 2003).

From a survey of 10 sources, in conjunction with the available literature, Kanekar & Chengalur (2003, hereafter KC03) find both detections and non-detections of 21-cm absorption in DLAs at $z < 2$, whereas the high- z results are almost exclusively non-detections (Fig. 1, top). Additionally, many of the $z < 1$ DLAs have host-galaxy identifications from optical imaging, given in Table 1. By combining the 21-cm optical depth with the total HI column density from optical spectroscopy covering the damped Lyman- α line, KC03 find low spin temperatures ($T_s \approx 200$ K), which are typical of the Milky Way and local spirals (Dickey & Lockman 1990), in all cases where the absorber was identified as a spiral (Fig. 1). Furthermore, all DLAs at $z < 1$ with temperatures $T_s \geq 1000$ K were found to be associated with dwarf or LSBs and KC03 interpreted the non-detections at high- z (> 2) as DLAs with high T_s . They therefore advocate a picture where the DLA host-galaxy population is dominated by the warmer dwarfs and LSBs at high- z and evolves to include a higher proportion of spirals at low- z , thus satisfying one expectation of hierarchical galaxy formation scenarios. However, in many of these studies, particularly at high redshift, the covering factor, f , of the background continuum is often assumed to be unity (Fig. 1, bottom – see also Table 1.). Since f plays an equal rôle as T_s in relating the column density to the observed optical depth profile, it is important to consider the robustness of this assumption, which is the aim of this article.

2 FACTORS AFFECTING THE DETECTION OF 21-CM ABSORPTION

2.1 Previous 21-cm absorption searches

In Table 1 we summarise the previously published 21-cm searches to which we add the 3 non-detections detailed in Appendix A. The optical depths are quoted for various resolutions between 0.6 and 17 km s^{-1} . As discussed in detail by Curran et al. (2002a), the choice of resolution affects the upper limit to the optical depth obtained and so we normalise these to 3 km s^{-1} , a fairly typical resolution for the DLAs detected in 21-cm absorption. In the table we also give the covering factors used to determine the spin temperature in each of the previous searches. Where no high resolution radio images are available for both the background source and absorber, it is common practice to assume that the absorber completely covers the continuum source (e.g. Lane & Briggs 2001), although in some cases the covering factor is estimated as the ratio of the compact unresolved component’s flux to the total radio flux (e.g. Briggs & Wolfe 1983). A good example of this method is given by Lane et al. (2000), where the constancy of the 21-cm absorption profile in the $z_{\text{abs}} = 0.09$ DLA over the partially resolved core of 0738+313 gives an estimate of $f \approx 0.98$. As Briggs & Wolfe (1983) mention, however, even though this method provides information on the background source structure, it provides none on the size of the absorbing region². The only way to unambiguously determine the covering factor is by mapping both the source and the absorbing gas at high angular resolution, which is challenging due to the very high sensitivities required.

2.2 Column density and background flux biases

In order to check that the non-detection of 21-cm absorption in DLAs is not the result of lower atomic hydrogen column densities, we plot the velocity integrated optical depth against column density in Fig. 2. We use this rather than the peak optical depth as this provides a better representation of the strength of the line. For a single cloud in thermodynamic equilibrium, the spin temperature of the gas can be estimated from the kinetic temperature according to $T_{\text{spin}} \approx T_{\text{kin}} \lesssim 22 \times \text{FWHM}^2$ (e.g. Lane & Briggs 2001) and this has been used by KC03 in order to derive spin temperatures and line-widths which are self consistent. However, in the absence of detailed knowledge of the covering factor, it is impossible to assign a specific spin temperature to the system. We therefore assume a FWHM of 20 km s^{-1} (the mean value of the detections) for the non-detections (Table 1). From the table see that the FWHM can range from 4 to 50 km s^{-1} , each of which would not cause too large a deviation from our chosen value of 20 km s^{-1} on the log plots. This is confirmed by the fact that using the peak rather than velocity integrated optical depths gives similar qualitative results in Figs. 2 and 3.

Although the column densities for the non-detections are generally lower, they appear to have been searched to correspondingly lower optical depth limits. To check this, in Fig. 3 we show the distribution of the velocity integrated optical depth modified according to the column density of each DLA: In the optically thin regime ($\sigma \ll f.S$) equation 1 reduces to³

² The effect of background source size is clearly demonstrated, for instance, in absorption studies of PSR B1849+00 (Stanimirovic et al. 2003).

³ As seen from Table 1, this is a reasonable assumption providing that f is

Table 1. The DLAs and sub-DLAs which have been searched for 21-cm absorption. In the top panel we list the detections and in the bottom panel the non-detections. τ_{peak} is the peak optical depth of each individually resolved component, the number of which are listed under n_{comp} (B designates a blend) and Δv is the full width half maximum (FWHM) of the line [km s^{-1}]. For the non-detections the 3σ upper limits of τ_{peak} at a velocity resolution of 3 km s^{-1} (see main text) are quoted. f and T_s are the covering factor used and the inferred spin temperature [K] from the literature, respectively. For the former \dagger denotes that f is estimated from high resolution radio images and * denotes that f is assumed. N_{HI} and z_{abs} are the total neutral hydrogen column density [cm^{-2}] (see <http://www.phys.unsw.edu.au/~sjc/dla/>) and the redshift of the DLA, respectively, with the optical identification (ID) given: D–dwarf, L–LSB, S–spiral, U–unknown. z_{em} is the redshift of the background QSO and S is the flux density [Jy] at ν_{obs} , obtained from either the reference given or as cited in Curran et al. (2002b). The final column gives the 21-cm absorption reference.

QSO	τ_{peak}	n_{comp}	Δv	f	T_{spin}	$\log N_{\text{HI}}$	z_{abs}	ID	z_{em}	S	Ref.
0235+164	0.7/0.5	3B+1	–	1 \dagger	100	21.7	0.52385	S	0.940	≈ 1.7	2
0248+430	0.2/0.2/0.1/0.1	4	–	1*	–	–	0.394	U	1.31	1.0	22
0458–020	0.3–3.1	2B	25	1–0.28 \dagger	< 1000	21.7	2.03945	U	2.286	3	7
0738+313	0.04	1	8	1 \dagger	1100	20.8	0.2212	D	0.635	1.9	14
...	0.25	2	4	0.98 \dagger	800	21.2	0.0912	U	...	2.2	19
0809+483 ^a	0.024	2B	35	–	–	20.2	0.4369	S	0.871	19.0	5
0827+243	0.007	1	50	0.67 \dagger	300	20.3	0.5247	S	0.939	0.9	20
0952+179	0.013	1	8	0.25 \dagger	2000	21.3	0.2378	L	1.472	1.4	20
1127–145	0.06,0.09	4B+1	42	1,1 \dagger	1000,910	21.7	0.3127	L	1.187	5.3,6.2	14,18
1157+014	0.05–0.2	1	42	0.25–1 \dagger	–	21.8	1.94362	L	1.986	0.80	4
1229–021	0.05	2B	5	0.43 \dagger	–	20.8	0.39498	S	1.045	2.2	6,13
1243–072	0.07	1	14	1*	–	–	0.4367	S	1.286	0.48	22
1328+307 ^b	0.11	1	8	0.2 \dagger	100	21.3	0.692154	S	0.849	19.0	1
1331+170	0.02	1	22	1*	980	21.2	1.77642	U	2.084	0.61	3
1413+135 ^c	0.3	1	18	≤ 0.1 \dagger	–	–	0.24671	S	0.24671	1.25	8
1629+120	0.039	2B	40	1 \dagger	20–310	20.7	0.5318	S	1.795	2.35	23
2351+456	0.32	1	53	–	–	–	0.779452	U	1.9864	2.0	24
0118–272	< 0.009	–	–	0.5 \dagger	> 850	20.3	0.5579	U	0.559	1.1	20
0201+113	0.09,0.04,< 0.09 ^d	1	9,23,–	1 \dagger	1100, ≥ 5000	21.3	3.386	U	3.610	0.35	11,12
0215+015	< 0.006	–	–	1 \dagger	> 1000	19.9	1.3439	U	1.715	0.92	23
0335–122	< 0.008	–	–	$\approx 1*$	> 3000	20.8	3.178	U	3.442	0.68	23
0336–017	< 0.007	–	–	1*	> 9000	21.2	3.0619	U	3.197	0.94	23
0432–440	–	–	–	–	–	20.8	2.297	U	2.649	–	25
0438–436	< 0.1	–	–	–	–	20.8	2.347	U	2.852	–	25
0439–433	< 0.012	–	–	1*	> 700	20.0	0.10097	U	0.593	0.33	21
0454+039	< 0.02	–	–	0.28 \dagger	–	20.7	0.8596	D	1.345	0.44	6
0528–250	< 0.3	–	–	1*	> 700	21.3	2.8112	U	2.779	0.14	10
0537–286	< 0.007	–	–	1 \dagger	> 1900	20.3	2.974	U	3.104	1.1	23
0906+430 ^e	< 0.01	–	–	–	–	–	0.63	U	0.670	6.14	17
0957+561A	< 0.01 ^f	–	–	–	–	20.3	1.391	U	1.413	0.59	23
1225+317	< 0.09	–	–	0.11 \dagger	–	–	1.821 ^g	U	2.219	0.35	6
1228–113	–	–	–	–	–	20.6	2.193	U	3.528	–	25
1354–107	< 0.07	–	–	1*	> 1000	20.8	2.996	U	3.006	0.12	23
1354+258	< 0.015 ^f	–	–	–	–	21.5	1.4205	U	2.006	0.30	23
1451–375	< 0.007	–	–	1*	> 1400	20.1	0.2761	U	0.314	3.8 ^h	18
2128–123	< 0.003	–	–	≈ 1 \dagger	> 1000	19.4	0.4298	U	0.501	1.9	23
2223–052 ⁱ	< 0.03	–	–	0.44 ^j	> 1600	20.9	0.4842	U	1.4040	8.0 ^h	18
2342+342	< 0.03	–	–	1*	> 4000	21.3	2.9084	U	3.053	0.31	23

Notes: ^a3C196, ^b3C286, ^cincluded by KC03, but since no Lyman- α absorption has been detected in this associated system we shall exclude it from our analysis, ^dalso, Briggs et al. (1997) detected 21-cm absorption with the WSRT but not the VLA; as with the current consensus (e.g. Wolfe, Gawiser & Prochaska 2003) we shall consider this a non-detection, ^e3C216 (although not detected in the Lyman- α line nor Mg II 2796/2803 Å doublet, the UV spectrum of Wills et al. (1995) suggests a possible DLA), ^fthese 3σ upper limits are not quoted in KC03 since the low core radio fluxes reduce the optical depth sensitivity as well as implying a low covering factor in both cases, ^gobserved at $z = 1.795$, ^hflux density estimated from neighbouring frequencies (see <http://www.phys.unsw.edu.au/~sjc/dla/>), ⁱ3C446, ^jalthough $f = 0.1$ is quoted by KC03 we find this to be 0.44 from Chengalur & Kanekar (2000).

References: (1) Brown & Roberts (1973), (2) Roberts et al. (1976), (3) Wolfe & Davis (1979), (4) Wolfe et al. (1981), (5) Brown & Mitchell (1983), (6) Briggs & Wolfe (1983), (7) Wolfe et al. (1985), (8) Carilli et al. (1992), (9) Lanzetta et al. (1995), (10) Carilli et al. (1996), (11) de Bruyn et al. (1996), (12) Kanekar & Chengalur (1997), (13) Briggs (1999), (14) Lane et al. (1998), (15) Rao & Turnshek (1998), (16) Chengalur & Kanekar (1999), (17) Pihlström et al. (1999), (18) Chengalur & Kanekar (2000), (19) Lane et al. 2000, (20) Kanekar & Chengalur (2001), (21) Kanekar et al. (2001), (22) Lane & Briggs (2001), (23) KC03, (24) Darling et al. (2004), (25) This paper (see Appendix A).

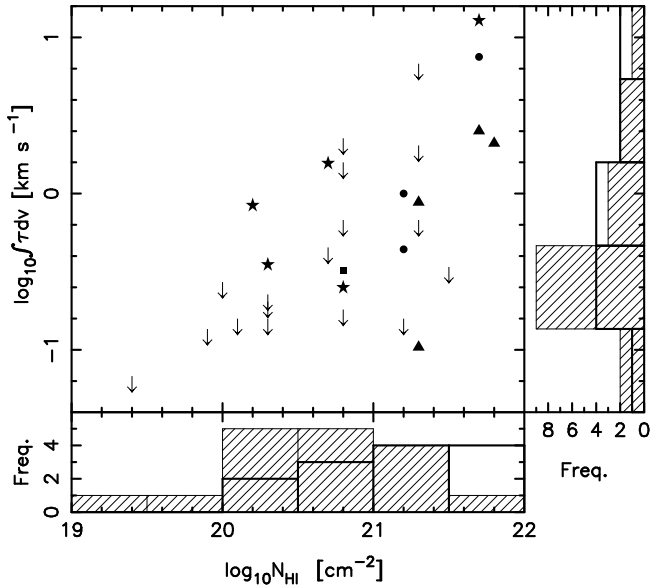


Figure 2. The velocity integrated optical depth versus total neutral hydrogen column density for the DLAs searched for 21-cm absorption. In this and the following figure, the shapes/bold histogram represent the detections and the arrows/hatched histogram the upper limits.

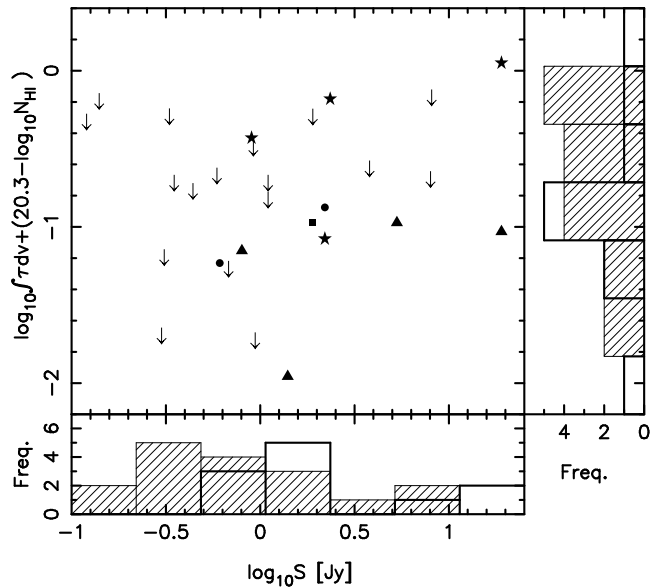


Figure 3. The modified velocity integrated optical depth versus the radio flux density at ν_{obs} for the optically thin ($\tau \lesssim 0.3$) 21-cm searches.

$$N_{\text{HI}} = 1.823 \times 10^{18} \frac{T_{\text{spin}}}{f} \int \frac{\sigma}{S} dv, \quad (2)$$

and from Table 1 we see that this is applicable ($\tau \lesssim 0.3$) to all but two systems, 0235+164 and 0458–020. With this approximation we can introduce a linear correction to the optical depth in order to account for the range of column densities exhibited by the DLA sample. Here we correct the optical depth by a factor of $2 \times 10^{20}/N_{\text{HI}}$, where $N_{\text{HI}} \geq 2 \times 10^{20} \text{ cm}^{-2}$ is nominally defined as the limiting

not small. For $f \lesssim \frac{\sigma}{0.3S}$ the assumption is not valid, although it supports the argument that $f \ll 1$.

column density of a DLA. This has the effect of putting the data points on an equal footing on the ordinate, i.e. for a given optical depth limit we account for the fact that a non-detected system of low column density has not been searched for as deeply as one of higher column density. From Fig. 3 we see, not surprisingly, that detections tend to occur towards higher flux densities, although the samples are not mutually exclusive. For the modified peak optical depths the overlap is more pronounced than in Fig. 3, and for both samples $-3 \lesssim \log_{10} \tau + [20.3 - \log_{10} N_{\text{HI}}] \lesssim -1.5$. Equation 2 therefore suggests similar values of f/T_{spin} (over a 2 order of magnitude range) for the detections and non-detections. We discuss the possible contributions of f and T_{spin} in the following section.

2.3 Spin temperatures and covering factors

From Section 2.2 it appears that neither the column density nor background flux (providing they are sufficiently high) are the main factors in determining whether a DLA is detected in 21-cm absorption. As previously discussed, the popular consensus is the wide range of estimated spin temperatures (possibly 20 to > 9000 K) in DLAs. In view that the equally influential covering factor is often assumed to be unity, we note the following:

(i) In radio quasar hosts the detection rate for 21-cm absorption is much higher in the compact sources, where the coverage is high (Pihlström et al. 2003; Vermeulen et al. 2003).

(ii) The presence of H_2 in 0528–020 (Levshakov & Varshalovich 1985) suggests that the gas is relatively cold with $T_{\text{kin}} \approx 200$ K (Srianand & Petitjean 1998), cf. $T_{\text{spin}} > 700$ K from a 21-cm non-detection (Carilli et al. 1996). This of course could be the result of different sight-lines being probed as well as the possibility the absorption is not due to a single cloud. This is known to be a complex situation with $z_{\text{abs}} \sim z_{\text{em}}$ (Table 1), suggesting an infalling system rather than a simple intervener, although it is one of the cases where a covering factor of unity is assumed. This is a valid assumption, however, if the absorbing material has an extent of $\gtrsim 70$ pc.⁴

Note that a similar situation is found towards 0738+313, where $T_{\text{kin}} \lesssim 300$ K, cf. $T_{\text{spin}} \approx 800$ K in both absorbers (Lane et al. 2000; Kanekar et al. 2001). As seen from the absorption profiles towards the 1.3 GHz VLBA image (figure 2 of Lane et al. 2000), although overall f is large, the coverage towards the north appears to be considerably less than towards the south-east. This suggests that the absorber extends to $\lesssim 16$ pc and ≈ 22 pc in these respective directions. A lower coverage in the northerly direction could possibly reduce the spin temperature estimates to closer to the kinetic temperature values, although the two-phase gas model suggested by Lane et al. (2000) offers an alternate explanation. In this model, the deep, narrow absorption lines give the temperature of the cold gas, and the much wider weaker line giving the warm gas temperature. These models are discussed further at the end of this section.

(iii) For the DLAs in which 21-cm absorption has been detected there appears to be little correlation between spin temperature and line-width. However, these are complex, multi-component systems characterised by a single velocity integrated optical depth and considering the possibility of both narrow/cold and wide/warm components in the profile (above), the lack of correlation is not surprising. Such simplification does however demonstrate the possible pitfalls in estimating line-widths for the non-detections (Section 2.2).

⁴ From the radio continuum size of $0.01''$ (see Table 2) at $z = 2.8$ ($H_0 = 75 \text{ km s}^{-1} \text{ Mpc}^{-1}$, $\Omega_{\text{matter}} = 0.27$).

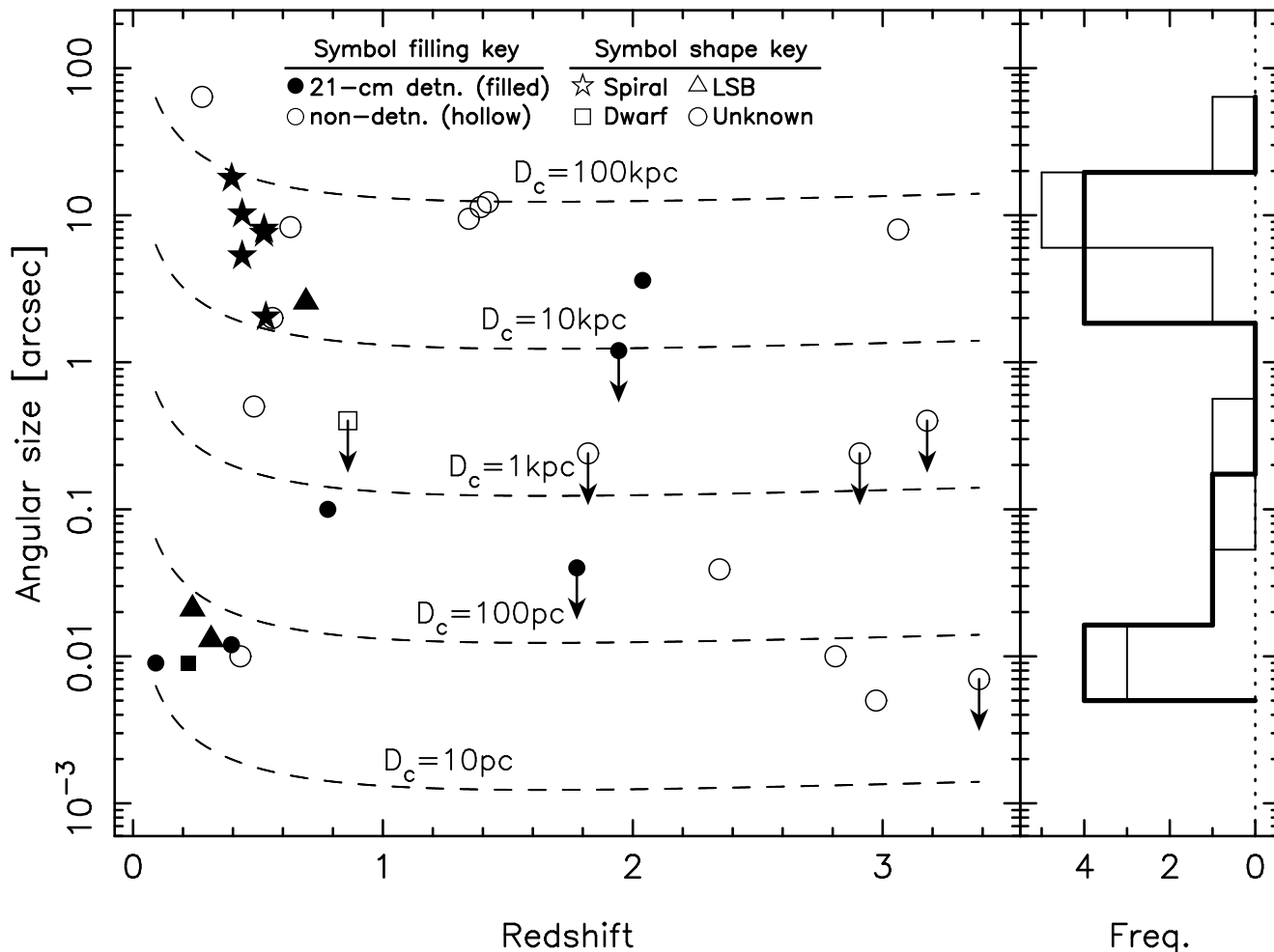


Figure 4. The angular sizes of the background radio continuum sources. Left: The dashed lines represent the angular extent of different size absorption clouds (D_c) as a function of redshift ($H_0 = 75 \text{ km s}^{-1} \text{ Mpc}^{-1}$, $\Omega_{\text{matter}} = 0.27$ and $\Omega_{\Lambda} = 0.73$). The source sizes are plotted at the absorption redshift. The arrows represent continuum source upper limits, the open symbols are the 21-cm non-detections and the solid symbols are the detections. Right: The frequency of various source sizes, where the bold histogram represents the detections (upper limits are excluded).

All 21-cm absorption detections occur in lower redshift ($z_{\text{abs}} \leq 2.04$) DLAs (see Fig. 4) and KC03 attribute this to these having a mix of both low and high spin temperatures (Fig. 1, top), while the higher redshift DLAs generally have high spin temperatures. This may imply that the more distant DLA sample consists of a particular class of object. However, due to their large distances, none of the high redshift 21-cm sample have hosts which have been optically identified and indeed only one of the $z < 2$ non-detections has an optical identification (Fig. 1, bottom). Therefore, we have insufficient information with which to determine the DLA host morphology and thus the likely covering factor. From this and the above points, we cannot rule out that perhaps the inferred (high) spin temperatures are an artifact of an overestimate of the covering factor.

One way to address this issue is to estimate how the expected size of the intervening absorber compares to that of the background continuum: In Table 2 we show the results from high resolution radio images for the sources searched⁵ and in Fig. 4 we

show the radio source size/absorption redshift distribution compared with various absorber sizes, D_c . Although we are uncertain which of these apply to a “typical” DLA (e.g. Briggs et al. 1989; Churchill & Charlton 1999; Chengalur & Kanekar 2002), the bimodal distribution of the continuum source sizes (particularly for the detections) itself may be indicative of a strong covering factor influence: Using the absorber host optical identifications for this sample we see a clear correlation between galaxy type and radio source size, where the spirals trace the upper segment ($\theta_{\text{QSO}} > 1''$) of the distribution and the compact galaxies appear to be associated with the smaller radio sources ($\theta_{\text{QSO}} < 0.2''$). The fact that absorption is detected only towards the extended continuum sources when occulted by a large galaxy strongly suggests that the covering factor is a key issue. Toward the smaller continuum sources we

table. Specifically, the flat SEDs for 0215+015, 0335–122 & 2342+342 suggest compact sources. For the remainder of their sources they use the ratio of the unresolved component’s flux (Section 2.1) to estimate the covering factor and, in order to avoid erroneous spin temperature estimates, exclude from further analysis the two sources (0957+561 & 1354+258) where this is expected to be low.

⁵ Note that the continuum source sizes estimated by KC03 from the spectral energy distributions (SEDs) agree qualitatively with the results in the

Table 2. Radio source sizes (arc-seconds) and VLBI and VLA morphologies of the QSOs illuminating DLAs searched for 21-cm absorption.

QSO	θ_{QSO}	Ref	VLBI	Ref	VLA	Ref	Comments [Ref]
0235+164	7.5	16	CJ	25	T	16	VLBI (5 GHz)/VLA (2 GHz) triple + extra strong component
0248+430	0.012	22	T	22	U	1	VLBI (1.6 GHz) weak core + 2 strong lobes or a CJ structure, outer J stronger than inner/VLA (5 GHz) < 0.8''
0458-020	3.6	38	CJ	30	CDom	38	VLBI (5 GHz)/VLA (5 GHz) core + weaker lobes (2 component, 1.4 GHz VLA [11])
0738+313	0.009	29	CJ/T	29	T	16	VLBI (5 GHz)/VLA (1.6 GHz) triple, FRI like (core strongest)
0809+483	5.27	3	-	-	D	3	VLA (5 GHz) FRII like (strong lobes), as MERLIN 408 MHz [23]
0827+243	8.00	17	CJ	39	D	17	VLBA (2 & 8 GHz)/VLA (1.4 GHz) FRII like
0952+179	0.021	39	T	39	-	-	VLBA (2 & 8 GHz) either CJ or C-J-CJ (one side stronger)
1127-145	0.013	24	CJ	24	U	1	VLBI/VLA (1.4 & 5 GHz)
1157+014	< 1.2	6	-	-	U	6	VLA (5 GHz)
1229-021	17.76	4	-	-	T	4	VLA standard triple, C + 2 weaker lobes
1243-072	10.17	5	CJ	39	T	5	VLBA (2 & 8 GHz)/VLA standard triple, core is dominant
1328+307	2.57	14	CJ	39	CDom	14	VLBA (2 & 8 GHz)/VLA (1.5 GHz) strong core + weaker component
1331+170	< 0.04	9,31	CJ	41	U	9	VLBA (2 & 8 GHz)/VLA (5GHz)
1413+135*	0.040	20	CJ	20	U	1	VLBI CJ + 2 more extended components on each side, core stronger VLA (5 GHz)
1629+120	2.025	15	D	32	T	15	VLBI (2 GHz) EVN/VLA 3 strong components, possibly FRII
2351+456	0.03	22	CJ	22	U	1	VLBI (1.7 GHz) strong 20-30 mas core + one weaker 100 mas jet
0118-272	2.0	1	T/mul	34	T/mul	2	VLBI (5 GHz) core + extended VLA (5 GHz) at least 3 components, complex
0201+113	< 0.007	32	C	32	CDom	12	Core + weak extended (1% of total 21-cm flux within 2'' [12])
0215+015	9.45	7	C	27	T	7	VLBA (2 & 8 GHz)/ VLA (5 GHz) FRI, core dominated
0335-122	< 0.4	11	C	41	U	11	VLBI (2 GHz)/VLA (1.4 GHz)
0336-017	8.0	37	CJ	18	T	37	VLBI (5 GHz) unresolved/VLA (5 GHz) FRI, core dominated
0432-440*	-	-	-	-	-	-	-
0438-436	0.039	35	D	35	U	1	VLBI (5 GHz)/VLA (1 & 5 GHz)
0439-433	-	-	-	-	-	-	-
0454+039	< 0.4	11	CJ	41	U	11	VLBA (2 & 8 GHz)/VLA (1 & 5 GHz)
0528-250	0.010	40	C	40	U	1	VLBI (5 GHz)/VLA (1 & 5 GHz)
0537-286	0.005	40	CJ	40	-	-	VLBA (2 & 8 GHz)
0906+430	8.3	14	CJ	22	T	14	VLBI (1.6 GHz) core strongest/VLA (1.4 GHz) core strongest
0957+561	11.36	28	CJ	21	T?	28	VLBI (5 GHz)/VLA (5 GHz) lensed, looks like CLL core strongest
1225+317	< 0.24	8	C	41	U	8	VLA (2 GHz) possibly CJ/VLA (5 GHz)
1228-113*	0.01	41	CJ	41	-	-	VLBA (2 & 8 GHz)/VLA: no map, may have flux on larger than VLBI scales
1354-107	-	-	-	-	-	-	-
1354+258	12.24	15	-	-	T	15	VLA (5 GHz) FRI like, core dominates
1451-375	63.79	33	CJ	39	T	33	VLBA (5 GHz)/VLA (1.4 GHz) FRI like, core dominates
2128-123	0.010	26	CJ	26	U	1	VLBA (2 & 8 GHz)/VLA (1 & 5 GHz)
2223-052	0.5	13	CJ	40	U	4	VLBA (2 & 8 GHz)/VLA (1.4 GHz)
2342+342	< 0.24	36	-	-	U	36	VLA (8 GHz)

Key VLBI morphology: CJ-core-jet morphology (most flux in core), D-double (2 lobes, no core visible), C-core, T-triple (core plus two lobes), mul = multiple components (> 3). N.B. it is not always possible to determine the core in the VLBI images.

Key VLA morphology: U-unresolved, T-triple, usually the morphology is either FRI like (most flux in core) or FRII like (most flux in lobes), D-double, usually FRII like (core may be too faint), CDom-core dominated, usually a very strong core plus some fainter emission (some may look like very weak lobes). *Note that these are included in order to provide a comprehensive list but not included in the analysis (Fig. 4) - 1413+135 is an associated system and the limits for 0432-440 and 1228-113 are poor (Appendix A)

References: (1) Ulvestad et al. (1981), (2) Perley (1982), (3) Schilizzi et al. (1982), (4) Hintzen et al. (1983), (5) Gower & Hutchings (1984), (6) Stocke et al. (1984), (7) Antonucci & Ulvestad (1985), (8) Rogora et al. (1987), (9) Barthel et al. (1988), (10) Briggs et al. (1989), (11) Neff & Hutchings (1990), (12) Stanghellini et al. (1990), (13) Fejes et al. (1992), (14) van Breugel et al. (1992), (15) Lonsdale et al. (1993), (16) Murphy et al. (1993), (17) Price et al. (1993), (18) Gurvits et al. (1994), (19) Lister et al. (1994), (20) Perlman et al. (1994), (21) Campbell et al. (1995), (22) Polatidis et al. (1995), (23) Reid et al. (1995), (24) Bondi et al. (1996), (25) Chu et al. (1996), (26) Fey et al. (1996), (27) Fey & Charlot (1997), (28) Harvanek et al. (1997), (29) Stanghellini et al. (1997), (30) Shen et al. (1997), (31) Browne et al. (1998), (32) Dallacasa et al. (1998), (33) Saikia et al. (1998), (34) Shen et al. (1998), (35) Tingay et al. (1998), (36) Wilkinson et al. (1998), (37) Reid et al. (1999), (38) Barthel et al. (2000), (39) Fey & Charlot (2000), (40) Fomalont et al. (2000), (41) Beasley et al. (2002).

would also expect spirals (together with compact galaxies) since the covering factor would also be large. This is not observed. KC03 do note that some of the identifications may be uncertain but, consulting the literature (e.g. Rao et al. 2003), we find similar identifications, although the morphology of the $z_{\text{abs}} = 0.09$ DLA towards 0738+313 is unclear (Cohen 2001) (this has therefore been flagged as unknown in Figs. 1, 4 and 5). The lower segment of the low redshift bimodal distribution therefore consists of 3 dwarf/LSBs and 3 unknowns⁶. That is, in this group there are as many compact as there are unidentified morphologies, though the latter could well turn out to be larger galaxies. Regarding the bimodal distribution, the binary probability of finding 6 out of 6 spiral galaxies towards sources of angular extent $\theta_{\text{QSO}} > 0.5''$ and 3 (or more) out of 4 non-spirals at $\theta_{\text{QSO}} < 0.5''$ is just 0.5 per cent. Thus, it would seem there is some evidence to suggest a non-negligible covering factor effect in the current sample.

Furthermore, as mentioned above, all but one of the non-detections at low redshift have yet to be identified optically, which excludes us from estimating a probable coverage, as done for the majority of the detections. However, in Fig. 4 we note that the low redshift DLAs not detected in 21-cm tend to occult the largest background sources. In fact 6 of these are located in the upper segment of the bimodal distribution, compared to only one in the lower segment⁷. This strongly suggests that the low redshift non-detections may be mainly due to inadequate coverage.

However, we emphasise one possible caveat to the above argument. Several of the larger ($\theta_{\text{QSO}} > 1''$) background sources have complex morphologies, and in fact for 6 of the non-detections (0215+015, 0336-017, 0906+430, 0957+561, 1354+258 & 1451-375) these may be core dominated (Table 2). The fact that there is no information on the core flux at the redshifted 21-cm frequency⁸ nor on the extent of the absorbing gas means that we cannot unambiguously attribute the non-detections purely to low covering factors, although the smallest continuum source size is $8''$ at ≥ 1.4 GHz.

One way to estimate the extent of the absorber required to fully cover the source is via the Compton limit of the emitting region, which places a lower limit on the size of the emitting region according to the upper limit of 10^{12} K for the brightness temperature (e.g. Rantakyro et al. 2003). Wolfe, Gawiser & Prochaska (2003) apply this to 0201+113, where $\theta_{\text{QSO}} < 7$ mas (Table 2), to obtain a minimum extent of 4.9 mas (or 35 pc at z_{abs} for $H_0 = 75 \text{ km s}^{-1} \text{ Mpc}^{-1}$, $\Omega_{\text{matter}} = 0.27$ and $\Omega_{\Lambda} = 0.73$). Applying this to the rest of the 21-cm sample gives 0.7–16 mas (or 1–130 pc at z_{abs}), all of which are small in comparison to θ_{QSO} . The results of Wolfe, Gawiser & Prochaska (2003) are interesting, however, since the extent of 0201+113 set by the Compton limit is very close to that set by the radio observations at 1.6 GHz ($< 2.5 \times 5.0 \text{ mas}^2$, Hodges et al. 1984; Stanghellini et al. 1990). From studies of the bolometric background radiation in DLAs, Wolfe, Prochaska & Gawiser (2003) find that these absorbers consist mainly of the cold neutral medium (CNM, where $T \sim 150$ K and $n \sim 10 \text{ cm}^{-3}$) rather than the warm neutral medium (WNM, $T \sim 8000$ K and $n \sim 0.2 \text{ cm}^{-3}$). This supports our argument for lower

covering factors and hence lower spin temperatures in DLAs, although based on the high covering factor towards 0738+313 (Section 2.1), Lane et al. (2000); Kanekar et al. (2001) suggest a two phase gas model dominated by the WNM ($\approx 75\%$) in both absorbers. This is consistent with the WNM+CNM mix in nearby dwarfs (Young et al. 2001, 2003), where such low metallicity systems are expected to reflect conditions in the early Universe, with the values of $[\text{O}/\text{H}] \sim 0.02$ to 0.2 solar (e.g. Lipovetsky et al. 1999; Lee et al. 2002) spanning the range of typical DLA metallicities up to $z_{\text{abs}} \sim 3.4$ (Prochaska et al. 2003; Curran et al. 2004). However, even with the warm gas contribution, the mean harmonic mean spin temperatures of ≈ 800 K towards 0738+313 still lie in the “cool DLA”, low redshift regime (Figs. 1 & 5, below).

In 0201+113 Wolfe, Gawiser & Prochaska (2003) find the CNM density to be $n \approx 6 \text{ cm}^{-3}$ and, by assuming that the total HI column density comprises several CNM (21-cm absorbing) clouds of column densities $N \approx 2 \times 10^{20} \text{ cm}^{-2}$, they obtain an estimate of $\lesssim 10$ pc for each CNM cloud. While this argument has the draw-back that the total HI column density in the CNM phase must be estimated, it leads to a range of possibilities for 0201+113, the two extremes of which are:

- (i) The $\lesssim 10$ pc 21-cm absorbing clouds are aligned with the line-of-sight towards the ≈ 40 pc (at z_{abs}) background continuum, so that the coverage is low but the total column density is high.
- (ii) The clouds are distributed with little overlap, giving high coverage but a low effective column density.

Having $f \sim 1$ and $N_{\text{CNM}} \ll N_{\text{HI}}$ could account for the 21-cm non-detections, while permitting a large fraction of CNM gas (Wolfe, Gawiser & Prochaska 2003). This emphasises how equation 1 can at best only provide a column density weighted mean harmonic spin temperature from a complex of clouds of various column densities, velocity dispersions and covering factors.

3 CONCLUSIONS

Upon a review of the literature, we suggest that less-than-complete covering factors may be at least partly responsible for the non-detection of 21-cm absorption in many DLAs. Although it is as important as the spin temperature in determining the column density of the absorber, the covering factor is at best estimated from insufficient data, and, more often than not, simply assumed to be unity. This assumption is prevalent in the high redshift cases, where high spin temperatures are claimed to be dominant, despite their being no DLA host identifications at $z_{\text{abs}} \gtrsim 0.9$.

Although all detections of 21-cm absorption occur at $z_{\text{abs}} \leq 2.04$, nearly half of those searched at these redshifts remain undetected, thus giving an apparent mix of both low and high spin temperatures for this sample. However, of these non-detections, ≈ 70 per cent of the absorbers occult large background radio sources ($\gtrsim 1''$), thus increasing the likelihood of $f < 1$. Furthermore, 21-cm absorption tends to be detected:

- (i) Towards large background sources ($> 1''$) only when the DLA is known to be associated with a large galaxy.
- (ii) Towards compact sources ($< 0.1''$) when the DLA is associated with an LSB or dwarf galaxy.

Naturally, we would also expect detections where the absorber is associated with a large spiral occulting a compact background continuum, thereby providing large coverage. However, this is not observed. Of the 6 detections towards small background sources, 3 of

⁶ Excluding the unknown at $0.1''$ & $z_{\text{abs}} = 0.779$ (2351+456). The $0.1''$ continuum size applies to the total extent, although the strong core flux originates within $\approx 0.03''$ (Polatidis et al. 1995) placing this closer to the other sources in this segment.

⁷ If applying the $\theta_{\text{QSO}} = 0.5''$ cut-off this becomes 7 versus 3.

⁸ These should, however, still provide a reasonable measure of the lower frequency source size (e.g. Fejes et al. 1992).

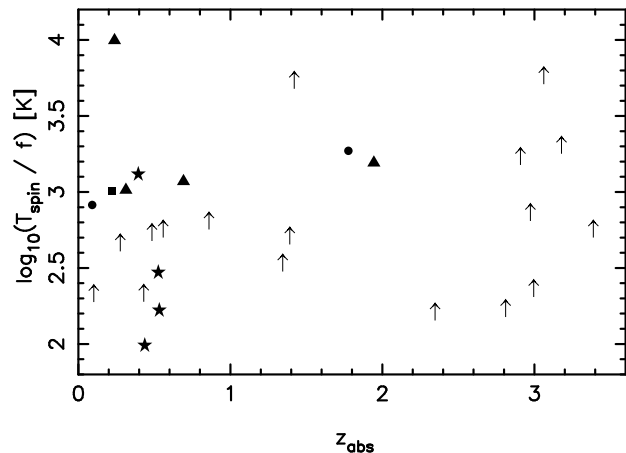


Figure 5. Spin temperature/covering factor ratio against absorption redshift for the optically thin ($\tau \lesssim 0.3$) 21-cm searches. Again the FWHM of the non-detections is assumed to be 20 km s^{-1} (Section 2.2).

the hosts are unidentified, thus not ruling out the possibility of an approximately equal mix of large and compact DLA hosts.

From the observed bolometric background, Wolfe, Gawiser & Prochaska (2003) propose that the 21-cm absorbing CNM is a major component of DLAs. They suggest that this is comprised of several lower column density clouds which may exhibit a large total column density but low covering factor when aligned along the line-of-sight or, conversely, low individual cloud column densities and a large covering factor, where overlap along the line-of-sight is minimal. Therefore, when attributing the non-detection of 21-cm absorption in DLAs to the effects of the covering factor (or spin temperature), we should bear in mind that the total HI column density may not provide a reliable estimate of the column density of the CNM along the line-of-sight to the background continuum. Further complications arise from the fact that insufficient detail is known about the flux contributions from the various components of the background continuum illuminating the DLA. The high resolution maps are at different frequencies than that of redshifted 21-cm and, if the components are extended, spectral indices may vary across them, making estimates of the effective continuum size at the appropriate frequency difficult. It is clear that high resolution observations at the appropriate frequencies are required in order to fully address this issue. Combining these with the absorption profiles at various locations over the background continuum (as in Lane et al. 2000) will give far better estimates of the covering factor.

Despite the above caveats, our analysis suggests that the covering factor may play an important rôle, thereby significantly lowering the spin temperature estimates of the DLAs for which the covering factors have been assumed (i.e. most of the non-detections) and perhaps it would be more prudent to use T_{spin}/f versus absorption redshift (Fig. 5) rather than just T_{spin} , for an unknown value of f . The figure does in fact show that the values of T_{spin}/f span similar ranges for both the detections and non-detections with the spirals (stars) being more concentrated towards the low T_{spin}/f (and z_{abs}) regime⁹ (although, as stated previously, the majority of host identifications are unknown). This is apparently consistent with the

⁹ Note however that the spread along the ordinate is considerably wider than in Fig. 1 (top): Over 1.2 dex in T_{spin}/f cf. 0.3 in T_{spin} . Arguably this is mainly influenced by 1229–021 at [0.39, 3.32] but also applies when we, as KC03, include the associated system 1413+135 at [0.25, 3.28].

interpretation of low spin temperatures in these objects (KC03), but also with high coverage by spirals, a possibility strongly suggested by the work presented here.

The lowering of covering factor estimates would introduce more uniformity to the spin temperatures of DLAs, while still supporting the hypothesis that large galaxies dominate the low redshift population (Baker et al. 2000) with dwarf galaxies constituting more of the high redshift population (Lanfranchi & Friaça 2003). That is, unlike KC03 who suggest that this is evident through increased spin temperatures at high redshift, we hypothesize that the absorption cross-sections of compact galaxies at these redshifts simply lack the extent to effectively cover the background radio continua.

ACKNOWLEDGMENTS

We wish to thank the referee, Wendy Lane, whose helpful comments improved the manuscript. Also, Matthew Whiting, Chris Blake, Rob Beswick, Nissim Kanekar, Fredrik Rantakyro, Sara Ellison and Panayiotis Tzanavaris for their helpful input and comments. We also wish to thank the John Templeton Foundation for supporting this work. SJC gratefully acknowledges receipt of a UNSW NS Global Fellowship and MTM is grateful to PPARC for support at the IoA under the observational rolling grant. This research has made use of the NASA/IPAC Extragalactic Database (NED) which is operated by the Jet Propulsion Laboratory, California Institute of Technology, under contract with the National Aeronautics and Space Administration.

REFERENCES

- Antonucci R. R. J., Ulvestad J. S., 1985, *ApJ*, 294, 158
- Baker A. C., Mathlin G. P., Churches D. K., Edmunds M. G., 2000, in Favata F., Kaas A., Wilson A., eds, *Star Formation from the Small to the Large Scale*, Vol.45 of ESA SP The Chemical Evolution of the Universe. Noordwijk, p. 21
- Barthel P. D., Miley G. K., Schilizzi R. T., Lonsdale C. J., 1988, *A&AS*, 73, 515
- Barthel P. D., Vestergaard M., Lonsdale C. J., 2000, *A&A*, 354, 7
- Beasley A. J., Gordon D., Peck A. B., Petrov L., MacMillan D. S., Fomalont E. B., Ma C., 2002, *ApJS*, 141, 13
- Bondi M., et al., 1996, *A&A*, 308, 415
- Briggs F. H., 1999, in Carilli C., Radford S., Menton K., Langston G., eds, *Highly Redshifted Radio Lines Redshifted 21cm Line Absorption by Intervening Galaxies*. ASP Conf. Ser., p. 16
- Briggs F. H., Brinks E., Wolfe A. M., 1997, *AJ*, 113, 467
- Briggs F. H., Wolfe A. M., 1983, *ApJ*, 268, 76
- Briggs F. H., Wolfe A. M., Liszt H. S., Davis M. M., Turner K. L., 1989, *ApJ*, 341, 650
- Brown R. L., Mitchell K. J., 1983, *ApJ*, 264, 87
- Brown R. L., Roberts M. S., 1973, *ApJ*, 184, L7
- Browne I. W. A., Wilkinson P. N., Patnaik A. R., Wrobel J. M., 1998, *MNRAS*, 293, 257
- Campbell R. M., Lehar J., Corey B. E., Shapiro I. I., Falco E. E., 1995, *AJ*, 110, 2566
- Carilli C. L., Lane W., de Bruyn A. G., Braun R., Miley G. K., 1996, *AJ*, 111, 1830
- Carilli C. L., Perlman E. S., Stocke J. T., 1992, *ApJ*, 400, L13
- Chen H.-W., Lanzetta K. M., 2003, *ApJ*, 597, 706
- Chengalur J. N., Kanekar N., 1999, *MNRAS*, 302, L29

- Chengalur J. N., Kanekar N., 2000, *MNRAS*, 318, 303
- Chengalur J. N., Kanekar N., 2002, *A&A*, 388, 383
- Chu L. B., Bååth F. T., Rantakyö F. J., Zhang H. S., Nicholson G., 1996, *A&A*, 307, 15
- Churchill C. W., Charlton J. C., 1999, *AJ*, 118, 59
- Cohen J. G., 2001, *AJ*, 121, 1275
- Curran S. J., Murphy M. T., Webb J. K., Rantakyö F., Johansson L. E. B., Nikolić S., 2002a, *A&A*, 394, 763
- Curran S. J., Webb J. K., Murphy M. T., Bandiera R., Corbelli E., Flambaum V. V., 2002b, *PASA*, 19, 455
- Curran S. J., Webb J. K., Murphy M. T., Carswell R. F., 2004, *MNRAS*, 351, L24
- Dallacasa D., Bondi M., Alef W., Mantovani F., 1998, *A&AS*, 129, 219
- Darling J., Giovanelli R., Haynes M. P., Bower G. C., Bolatto A. D., 2004, *ApJ*, 613, L101
- de Bruyn A. G., O’Dea C. P., Baum S. A., 1996, *A&A*, 305, 450
- Dickey J. M., Lockman F. J., 1990, *ARA&A*, 28, 215
- Ellison S. L., Yan L., Hook I. M., Pettini M., Wall J. V., Shaver P., 2001, *A&A*, 379, 393
- Fejes I., Porcas R. W., Akujor C. E., 1992, *A&A*, 257, 459
- Fey A. L., Charlot P., 1997, *ApJS*, 111, 95
- Fey A. L., Charlot P., 2000, *ApJS*, 128, 17
- Fey A. L., Clegg A. W., Fomalont E. B., 1996, *ApJS*, 105, 299
- Fomalont E. B., Frey S., Paragi Z., Gurvits L. I., Scott W. K., Taylor A. R., Edwards P. G., Hirabayashi H., 2000, *ApJS*, 131, 95
- Gower A. C., Hutchings J. B., 1984, *AJ*, 89, 1658
- Gurvits L. I., Schilizzi R. T., Barthel P. D., Kardashev N. S., Kellermann K. I., Lobanov A. P., Pauliny-Toth I. I. K., Popov M. V., 1994, *A&A*, 291, 737
- Haehnelt M. G., Steinmetz M., Rauch M., 1998, *ApJ*, 495, 647
- Harvanek M., Stocke J. T., Morse J. A., Rhee G., 1997, *AJ*, 114, 2240
- Hintzen P., Ulvestad J., Owen F., 1983, *AJ*, 88, 709
- Hodges M. W., Mutel R. L., Phillips R. B., 1984, *AJ*, 89, 1327
- Kanekar N., Chengalur J. N., 1997, *MNRAS*, 292, 831
- Kanekar N., Chengalur J. N., 2001, *A&A*, 369, 42
- Kanekar N., Chengalur J. N., 2003, *A&A*, 399, 857
- Kanekar N., Chengalur J. N., Subrahmanyan R., Petitjean P., 2001, *A&A*, 367, 46
- Kanekar N., Ghosh T., Chengalur J. N., 2001, *A&A*, 373, 394
- Lane W., Smette A., Briggs F. H., Rao S. M., Turnshek D. A., Meylan G., 1998, *AJ*, 116, 26
- Lane W. M., Briggs F. H., 2001, *ApJ*, 561, L27
- Lane W. M., Briggs F. H., Smette A., 2000, *ApJ*, 532, 146
- Lanfranchi G. A., Friaça A. C. S., 2003, *MNRAS*, 343, 481
- Lanzetta K. M., Wolfe A. M., Turnshek D. A., 1995, *ApJ*, 440, 435
- Lanzetta K. M., Wolfe A. M., Turnshek D. A., Lu L., McMahon R. G., Hazard C., 1991, *ApJS*, 77, 1
- Le Brun V., Bergeron J., Boissé P., Deharveng J. M., 1997, *A&A*, 321, 733
- Lee H., Grebel E. K., Hodge P. W., 2002, *BAAS*, 34, 1121
- Levshakov S. A., Varshalovich D. A., 1985, *MNRAS*, 212, 517
- Lipovetsky V. A., Chaffee F. H., Izotov Y. I., Foltz C. B., Kniazev A. Y., Hopp U., 1999, *ApJ*, 519, 177
- Lister M. L., Gower A. C., Hutchings J. B., 1994, *AJ*, 108, 821
- Lonsdale C. J., Barthel P. D., Miley G. K., 1993, *ApJS*, 87, 63
- Murphy D. W., Browne I. W. A., Perley R. A., 1993, *MNRAS*, 264, 298
- Neff S. G., Hutchings J. B., 1990, *AJ*, 100, 1441
- Perley R. A., 1982, *AJ*, 87, 859
- Perlman E. S., Stocke J. T., Shaffer D. B., Carilli C. L., Ma C., 1994, *ApJ*, 424, L69
- Pihlström Y. M., Conway J. E., Vermeulen R. C., 2003, *A&A*, 404, 871
- Pihlström Y. M., Vermeulen R. C., Taylor G. B., Conway J. E., 1999, *ApJ*, 525, L13
- Polatidis A. G., Wilkinson P. N., Xu W., Readhead A. C. S., Pearson T. J., Taylor G. B., Vermeulen R. C., 1995, *ApJS*, 98, 1
- Price R., Gower A. C., Hutchings J. B., Talon S., Duncan D., Ross G., 1993, *ApJS*, 86, 365
- Prochaska J. X., Gawiser E., Wolfe A. M., Castro S., Djorgovski S. G., 2003, *ApJ*, 595, L9
- Prochaska J. X., Wolfe A. M., 1997, *ApJ*, 487, 73
- Rantakyö F. T., Wiik K., Tornikoski M., Valtaoja E., Bååth L. B., 2003, *A&A*, 405, 473
- Rao S., Nestor D. B., Turnshek D., Lane W. M., Monier E. M., Bergeron J., 2003, *ApJ*, 595, 94
- Rao S. M., Turnshek D. A., 1998, *ApJ*, 500, L115
- Reid A., Shone D. L., Akujor C. E., Browne I. W. A., Murphy D. W., Pedelty J., Rudnick L., Walsh D., 1995, *A&AS*, 110, 213
- Reid R. I., Kronberg P. P., Perley R. A., 1999, *ApJS*, 124, 285
- Roberts M. S., Brown R. L., Brundage W. D., Rots A. H., Haynes M. P., Wolfe A. M., 1976, *AJ*, 81, 293
- Rogora A., Padrielli L., de Ruiter H. R., 1987, *A&AS*, 67, 267
- Ryan-Weber E. V., Webster R. L., Staveley-Smith L., 2003, *MNRAS*, 343, 1195
- Saikia D. J., Holmes G. F., Kulkarni A. R., Salter C. J., Garrington S. T., 1998, *MNRAS*, 298, 877
- Schilizzi R. T., Kapahi V. K., Neff S. G., 1982, *JA&A*, 3, 173
- Shen Z.-Q., Wan T.-S., Moran J. M., Jauncey D. L., Reynolds J. E., Tzioumis A. K., 1997, *AJ*, 114, 1999
- Shen Z.-Q., Wan T.-S., Moran J. M., Jauncey D. L., Reynolds J. E., Tzioumis A. K., 1998, *AJ*, 115, 1357
- Srianand R., Petitjean P., 1998, *A&A*, 335, 33
- Stanghellini C., Baum S. A., O’Dea C. P., Morris G. B., 1990, *A&A*, 233, 379
- Stanghellini C., O’Dea C. P., Baum S. A., Dallacasa D., Fanti R., Fanti C., 1997, *A&A*, 325, 943
- Stanimirovic S., Weisberg J. M., Dickey J. M., de la Fuente A., Devine K., Hedden A., Anderson S. B., 2003, in *Magnetic Fields and Star Formation: Theory Versus Observations PSR B1849+00 probes the tiny-scale molecular gas?* Kluwer
- Stocke J. T., Foltz C. B., Weymann R. J., Christiansen W. A., 1984, *ApJ*, 280, 476
- Tingay S. J., et al., 1998, *ApJ*, 497, 594
- Turnshek D. A., Wolfe A. M., Lanzetta K. M., Briggs F. H., Cohen R. D., Foltz C. B., Smith H. E., Wilkes B. J., 1989, *ApJ*, 344, 567
- Ulvestad J., Johnston K., Perley R., Fomalont E., 1981, *AJ*, 86, 1010
- van Breugel W. J. M., Fanti C., Fanti R., Stanghellini C., Schilizzi R. T., Spencer R. E., 1992, *A&A*, 256, 56
- Vermeulen R. C., et al., 2003, *A&A*, 404, 861
- Wilkinson P. N., Browne I. W. A., Patnaik A. R., Wrobel J. M., Sorathia B., 1998, *MNRAS*, 300, 790
- Wills B. J., et al., 1995, *ApJ*, 447, 139
- Wolfe A. M., 1980, *Physica Scripta*, 21, 744
- Wolfe A. M., Briggs F. H., Jauncey D. L., 1981, *ApJ*, 248, 460
- Wolfe A. M., Briggs F. H., Turnshek D. A., Davis M. M., Smith H. E., Cohen R. D., 1985, *ApJ*, 294, L67
- Wolfe A. M., Burbidge G. R., 1975, *ApJ*, 200, 548
- Wolfe A. M., Davis M. M., 1979, *AJ*, 84, 699

Table 3. The known southern radio illuminated DLAs and sub-DLAs which fall into the Parkes 70-cm receiver band (B1950.0 names are used throughout this paper). These are obtained from Turnshek et al. (1989)^a, Lanzetta et al. (1991)^b and Ellison et al. (2001)^c, where N_{HI} and z_{abs} are the column density (cm^{-2}) and the redshift of the DLA, respectively. ν_{obs} is the observed frequency of the redshifted 21-cm line (MHz) and S is the flux density of the background QSO at this frequency in Jy (see Curran et al. 2002). For 0528–2505 the value is the flux at 372 MHz (Carilli et al. 1996) and for 1228–113 the value is from a 327 MHz Giant Metrewave Radio Telescope (GMRT) observation (Nissim Kanekar, private communication).

QSO	$\log N_{\text{HI}}$	z_{abs}	ν_{obs}	S
0432–440 ^c	20.8	2.297	430.82	0.72
0438–436 ^c	20.8	2.347	424.38	8.10
0528–250 ^b	20.6	2.1410	452.65	0.14
1017+109 ^b	19.9	2.380	420.24	1.43
1021–006 ^{a,b}	19.6	2.398	418.01	0.50
1228–113 ^c	20.6	2.193	444.85	0.35
2136+141 ^a	19.8	2.134	453.22	0.76

- Wolfe A. M., Gawiser E., Prochaska J. X., 2003, *ApJ*, 593, 235
Wolfe A. M., Prochaska J. X., Gawiser E., 2003, *ApJ*, 593, 215
Young L. M., van Zee L., Dohm-Palmer R. C., Lo K. Y., 2001, in Hibbard J. E., R. M., van Gorkom J. H., eds, *Gas and Galaxy Evolution Star Formation and the Interstellar Medium in Dwarf Galaxies*. ASP Conf. Ser., Vol 240, San Francisco, p. 187
Young L. M., van Zee L., Lo K. Y., Dohm-Palmer R. C., Beierle M. E., 2003, *ApJ*, 592, 111

This paper has been typeset from a $\text{\TeX}/\text{\LaTeX}$ file prepared by the author.

APPENDIX A

Our initial motivation for this work was a search for 21-cm absorption in DLAs with the Parkes radio telescope. From the September 2001 version of our catalogue of all known DLAs (Curran et al. 2002)¹⁰ we shortlisted those which are illuminated by radio-loud QSOs (i.e. those with a measured radio flux density $\gtrsim 0.1$ Jy). From these, the DLAs with redshifts appropriate to the Parkes 70-cm receiver bandwidth (i.e. $2.1 \lesssim z \lesssim 2.4$) known to occult southern ($\delta < 30^\circ$) QSOs were selected (Table 3). Although there are 7 possible targets, we used the 90 hours scheduled to concentrate on 3 of the 4 confirmed DLAs; 0432–440, 0438–436 & 1228–113¹¹. 0528–250 was excluded due to its relatively low flux density. The redshifts of these DLAs are known to within $\Delta z \approx \pm 0.002$ (Sara Ellison, private communication), corresponding to $\Delta \nu \approx \pm 0.25$ MHz ($\approx \pm 200$ km s⁻¹).

The observations were undertaken in January 2002 using the 70-cm receiver on the Parkes 64-m antenna. We used the AT conversion system with the multibeam correlator, giving a bandwidth of 8 MHz ($\Delta z \approx \pm 0.03$) over 2048 channels (i.e. a spectral dispersion of 2.8 km s⁻¹ per channel) and position switching with 1° beam throw. The weather was clear and dry giving system temperatures typically between 60 and 150 K. Although

we restricted our observations to night time, we experienced severe radio-frequency interference (RFI) in this band. The RFI consisted primarily of sharp (FWHM $\lesssim 6$ km s⁻¹) ‘spikes’ and broad (FWHM $\gtrsim 100$ km s⁻¹) ‘humps’. The humps in particular were found to shift in frequency between 120-s scans of the on- and off-source positions. Therefore, attempts to subtract the off-source scans from their corresponding on-source scans merely introduced strong RFI variations in the residual spectrum with characteristic length scales ≈ 30 km s⁻¹, i.e. the very scales typical of HI 21-cm absorption lines in DLAs (see Table 2). The stronger spikes were also often accompanied by a powerful ‘ringing’ such that strong correlations between neighbouring channels could be seen to die away over ≈ 300 km s⁻¹ scales. The data reduction was therefore carried out using software written specifically for the purpose of dealing with this RFI. The reduction steps are summarised as follows:

- (i) The off-source scans were discarded and the on-source scans were low-pass filtered to provide a basic continuum shape which included the humps but ignored the spikes. The filtering scale was set so that ≈ 50 km s⁻¹ absorption features could be recovered reliably. This continuum was then subtracted from the on-source scans leaving relatively flat residual spectra contaminated by the spikes.
- (ii) For each QSO, all $\gtrsim 500$ contributing scans were corrected to the heliocentric frame and re-dispersed to a common frequency scale with a dispersion of 10 km s⁻¹.
- (iii) A 1σ error array was constructed for each re-dispersed scan based on the rms in a sliding 20-channel window and channels with fluxes deviating by more than 3σ were flagged and ignored in further reduction steps.
- (iv) Finally, the fluxes in corresponding channels in each scan were median filtered, values more than 2σ from the median rejected and the remaining values combined to form the weighted mean flux density and 1σ error arrays.

In Fig. 6 we show the resulting spectra for each DLA. It is clear that there are no significant, convincing absorption features over the mitigated intervals covered by the spectra (which include the frequencies expected from the optical redshifts). Generally, the noise level is quite high, ≈ 0.1 – 0.2 Jy (cf. the theoretical value of $\sigma \lesssim 3$ mJy per 10 km s⁻¹ channel) and some regions of the spectra were so severely affected by RFI that the errors are higher still. Where no reliable data could be gathered from any of the contributing scans, we have assigned a normalized flux density of zero and an effectively infinite error. Note also that the low-pass filter applied in stage (i) of the reduction procedure effectively prevents us from detecting absorption features with FWHM $\gtrsim 100$ km s. The 3σ optical depth limits quoted in Table 1 for these sources must therefore carry these caveats.

Due to the severe RFI, no flux densities could be obtained for our sources. Using the values in Table 3, for $\sigma = 0.2$ Jy at 10 km s⁻¹ resolution we obtain no 3σ detection of the flux for either 0432–440 nor 1228–113 and $\tau < 0.1$ for the optical depth of 21-cm absorption in the DLA towards 0438–436. From equation 2 and the column density of the Lyman- α line (Table 1), this gives $\frac{T_{\text{spin}}}{f} \times \text{FWHM} \gtrsim 3500$ K km s⁻¹, i.e. $\frac{T_{\text{spin}}}{f} \gtrsim 1200$ K per 3 km s⁻¹ channel or $T_{\text{s}} \gtrsim 200$ K for a FWHM of 20 km s⁻¹ (see Section 2.2).

¹⁰ A version of this catalogue is continually updated on-line and is available from <http://www.phys.unsw.edu.au/~sjc/dla>

¹¹ 1017+109, 1021–006 and 2136+141 are candidate DLAs which have yet to be confirmed using high resolution optical spectroscopy.

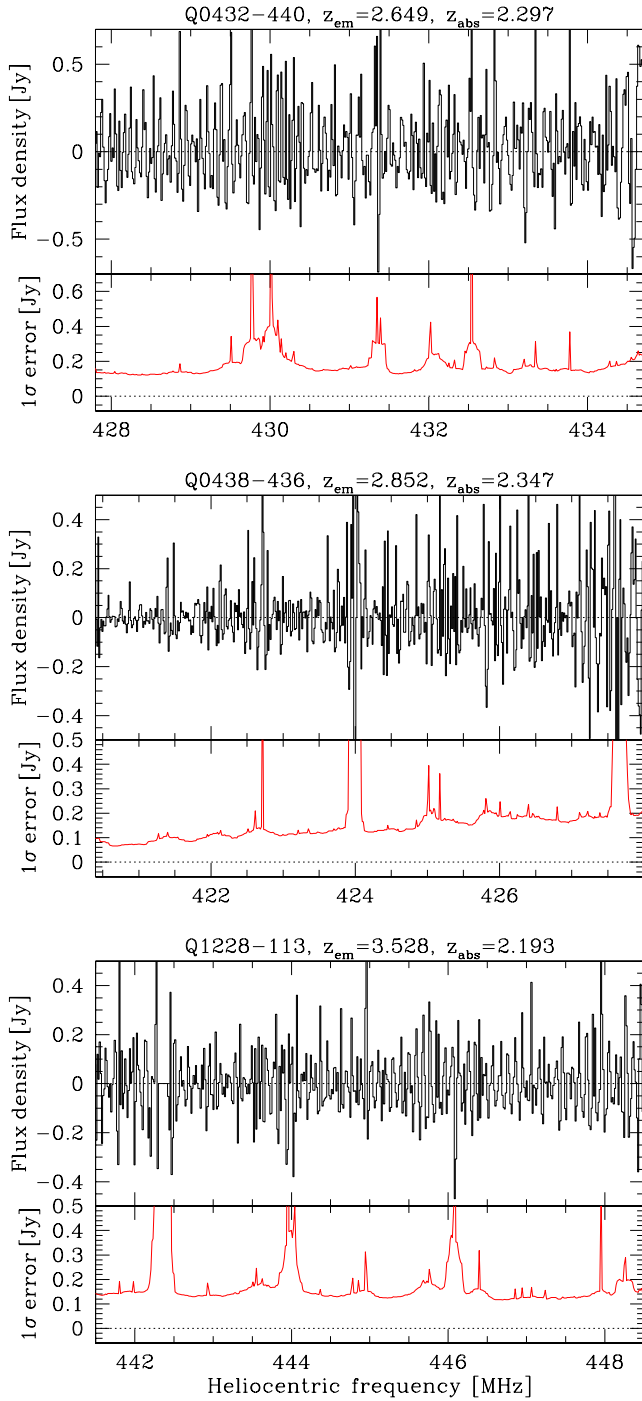


Figure 6. Parkes 21-cm spectra towards 0432–440 (top), 0438–436 (middle) and 1228–113 (bottom). An uncertainty of $\Delta z \approx \pm 0.002$ corresponds to the ranges 430.6–431.1, 424.1–424.6 and 444.6–445.1 MHz, respectively, indicating that spikes have been successfully removed over the ranges expected from the optical absorption.